



METHOD PAPER

New palaeocurrent analysis approach from two-dimensional trough cross-strata using photographs and anisotropy of magnetic susceptibility

Jasper Maars¹ | Gijs van Dijk¹ | Mark J. Dekkers¹ | F. Javier Hernández-Molina² | Federico Andreetto¹ | Francisco J. Rodríguez-Tovar³ | Wout Krijgsman¹

¹Department of Earth Sciences, Utrecht University, Utrecht, The Netherlands

²Drifters Research Group, Department of Earth Sciences, Royal Holloway University, London, UK

³Departamento de Estratigrafía y Paleontología, Universidad de Granada, Granada, Spain

Correspondence

Jasper Maars, Montaubanstraat 30, 3701 HR Zeist, The Netherlands.
Email: jasper.maars@tno.nl

Funding information

Horizon Europe 2020: Grant/Award Number: 765256

Abstract

Palaeocurrent analysis is vital for basin analysis and helps in the interpretation of depositional environments (along-slope or downslope). For that, it is crucial to have multiple measuring methods at hand to apply palaeocurrent analysis with a wide range of different datasets (outcrops, cores and photographs). Here, two relatively underexploited palaeocurrent measurement techniques are assessed when applied to trough cross-stratification observed in the Arenazzolo Formation at Eraclea Minoa (Sicily). The first technique is a novel design of a qualitative approach to infer palaeocurrent directions from photographs of two-dimensional sedimentary structures. The second technique involves measurements of the anisotropy of magnetic susceptibility from drilled samples. A broad agreement, with overlapping uncertainty boundaries, is observed between results from both techniques. This agreement validates the use of trough cross-strata to infer palaeocurrent directions. Moreover, the addition of photographs improves reproducibility and prevents a bias towards the best-exposed troughs. The application of both techniques to outcrops and sedimentary cores provides new opportunities for palaeocurrent analysis in any type of sedimentary environment.

KEYWORDS

analysis, anisotropy of magnetic susceptibility, magnetic fabric, palaeocurrent, phyllosilicates, trough cross-stratification

1 | INTRODUCTION

Palaeocurrent analysis is an important tool for basin analysis (Potter & Pettijohn, 2012) in the reconstruction of sediment-routing systems (Jipa & Olariu, 2013) and for provenance analysis (Amajor, 1987; Zhao et al., 2020). In addition, palaeocurrent directions can be crucial for

interpreting the depositional environment of a sedimentary deposit (e.g. along-slope vs. downslope currents). Palaeocurrent analysis is often based on cross-stratification for which three-dimensional structures and a sufficient number of measurements are required. Therefore, conventional palaeocurrent analysis in the field is often problematic since proper three-dimensional structures

This is an open access article under the terms of the [Creative Commons Attribution](https://creativecommons.org/licenses/by/4.0/) License, which permits use, distribution and reproduction in any medium, provided the original work is properly cited.

© 2024 The Authors. *The Depositional Record* published by John Wiley & Sons Ltd on behalf of International Association of Sedimentologists.

are scarcely exposed. To tackle this problem, DeCelles and Langford (1983) developed a qualitative technique to infer palaeocurrent directions from two-dimensional sedimentary structures. Despite its potential, this technique has experienced only limited field application. Here, this technique is optimised by integrating the use of photographs taken perpendicular to outcrops. The major asset of using photographs is that they prevent a bias towards the clearest exposed troughs. In addition, measurements are not limited by the available time in the field, and reproducibility is enhanced. Here, this trough cross-strata photographic method is validated with the anisotropy of magnetic susceptibility (AMS) approach as an independent technique for inferring palaeocurrent directions.

1.1 | Geological setting

Studied outcrops are located on Sicily, along the coast near Eraclea Minoa (37.391° N, 13.279° E). The outcrops are exposed by tectonic uplift related to the development of the Sicilian fold-and-thrust belt. The youngest structural unit of this fold-and-thrust belt is the southward-migrating Gela Nappe (Lickorish et al., 1999; Butler et al., 2019). The Gela Nappe hosts the Caltanissetta Basin which was filled by a thick sedimentary succession of Messinian deposits (Hsü et al., 1973; Roveri et al., 2014). This succession includes shales, sands and gypsum of the informal Pasquasia Formation (Selli, 1960) or upper gypsum (UG) (Manzi et al., 2009). The uppermost part of this UG consists of the latest Messinian Arenazzolo Formation (Manzi et al., 2009); an *ca* 8 m thick sandy unit directly underlying the official base of the Pliocene series and Zanclean stage. The global boundary stratotype section and point of the Zanclean was defined at the Eraclea Minoa section (Van Couvering et al., 2000).

The Arenazzolo Formation has been linked to a small deltaic system (Schreiber et al., 1976; Roveri et al., 2008; Manzi et al., 2009) at the edge of a lake (Cita & Colombo, 1979) when the Mediterranean was disconnected from the Atlantic Ocean. Others have proposed that the Arenazzolo Formation is a transgressive sequence, linked to the Zanclean reflooding of the Mediterranean (Broksma, 1978; Londeix et al., 2007; Bache et al., 2012; Popescu et al., 2021). Recently, it was interpreted as an along-slope contouritic deposit, based on palaeocurrent directions among other criteria, related to a terminal Messinian flooding event (Van Dijk et al., 2023). Two trough cross-stratified cosets of the Arenazzolo Formation that are exposed in two coastal outcrops with an 80° angle between them are analysed here (Figure 1). This mutual angle provides an excellent setting to test and compare both palaeocurrent analysis techniques.



FIGURE 1 Aerial image of the study area (37°23'28" N, 13°16'45" E) indicating two studied outcrops at Eraclea Minoa (ERA and ERB). Basemap source: ArcGIS World imagery basemap; ESRI 2016. Nov. 19–2022.

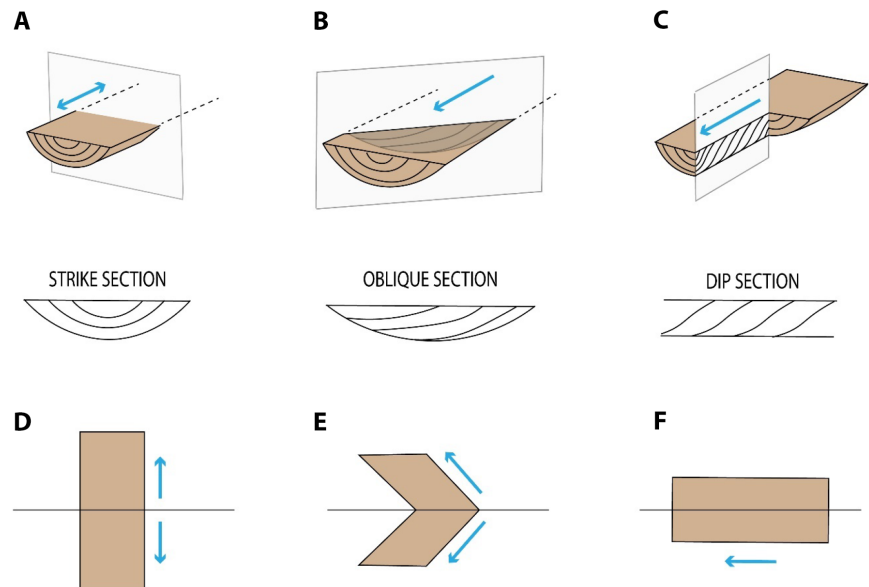
2 | EXISTING METHODS FOR PALAEOCURRENT DETERMINATION

2.1 | Geometry of various trough cross-sections

The conventional method for palaeocurrent determination using trough or tabular cross-stratification is by the measurement of foreset planar surfaces. Cross-stratification (tabular and trough) results from the downcurrent migration of dunes, bars or ripples (Hamblin, 1961; Allen, 1963; Harms et al., 1975). Sinuous-crested bedforms develop trough cross-stratification where the trough axes generally correspond to the flow direction. The trough is a semicylinder (Figure 2) that narrows down to a steeply plunging scoop-shape, upcurrent at the end of the trough (Slingerland & Williams, 1979; DeCelles & Langford, 1983). Within the trough, foreset fronts accumulate in the down current direction and form the infilling laminae. Hence, the downdip direction of the infilling laminae indicates the palaeocurrent direction, assuming a symmetrical infill. To account for the natural variability in the downdip directions, a statistically sufficient large dataset (*ca* 30) is required.

A set of trough cross-strata has curved laminae that are symmetrically dispersed with respect to the trough axis. Therefore, a section perpendicular to the trough axis, the strike section, has symmetrical semi-ellipsoidal truncations (Figure 2A). The other end-member section parallel to the trough axis, the dip section, has straight or tangential truncations of the successive foresets (Figure 2C). All other possible sections have their geometry somewhere in between. For example, an oblique section at a 45° angle to the trough axis has non-symmetrical curved laminae truncated by the lowermost set boundary (Figure 2B). The relationship between the geometry of the laminae and the

FIGURE 2 Trough cross-strata sections exposed at a vertical cut from various angles and cross-section views. (A) Perpendicular view, (B) oblique view at 45° and (C) parallel view. (D–F) Plan view of trough cross-strata sets. The blue arrows indicate the directions of the palaeocurrent that can be derived from each geometry.



plane of the section at which the trough is exposed can be exploited to recover the trough axis and thereby estimate palaeocurrent directions (DeCelles & Langford, 1983).

The relationship between the geometry of the truncated foresets and the palaeocurrent direction varies for each section. A section perpendicular to the trough axis (strike section) indicates two possible palaeocurrent directions parallel to the trough axis (Figure 2D). Alternatively, a section parallel to the trough axis (dip section) yields only one possible current direction in vertical outcrops, the downdip direction of the successive foresets (Figure 2F). For oblique sections two possible palaeocurrent directions can be inferred, each mutually at the same angle with to the plane of view (Figure 2E). The relationship between palaeocurrent directions and the two-dimensional vertical sections is best visualised with a bird's-eye view of the vertical section and an imaginary mirror plane through the trough (Figure 2D,E,F).

2.2 | Anisotropy of magnetic susceptibility

Anisotropy of magnetic susceptibility is a proxy for grain fabric and is a commonly used method for bulk three-dimensional determination of grain orientation (Channell et al., 1979; Baas et al., 2007). Comparison with petrographic techniques demonstrated an overall agreement between petrographic fabric and magnetic fabric (Taira & Lienert, 1979). When a fabric contains a preferred orientation of long grain axes, the fabric is anisotropic; with randomly oriented grains the fabric is isotropic (Pettijohn, 1975; Collinson & Thompson, 1982). In a sedimentological context, a preferred orientation (i.e. anisotropic fabric) can be produced by currents affecting the

grains during deposition. When ferromagnetic or paramagnetic minerals are present, the hydrodynamically generated grain fabric is represented by the magnetic fabric which can be measured. Therefore, AMS has been used to estimate palaeocurrent directions from both drill cores (Ellwood & Ledbetter, 1979; Hassold et al., 2006; Parés et al., 2007) and exposures (Crimes & Oldershaw, 1967; Hiscott & Middleton, 1980; Piper et al., 1996; Felletti et al., 2016). The AMS of rocks is represented by a second-order tensor, visualised as an ellipsoid having three principal axes (K_{\max} , K_{int} , K_{\min}) in a Cartesian coordinate system (Borradaile, 1991). The AMS ellipsoid can be described by various AMS parameters (Tarling & Hrouda, 1993). The corrected anisotropy degree (P_j), which describes the degree of alignment relative to the bulk susceptibility (K_m), the foliation parameter (F), which describes the degree of bedding-parallel alignment, and the lineation parameter (L), which describes the alignment in a specific direction (Jelinek, 1981), are used here.

3 | METHODOLOGY FOR A NOVEL TECHNIQUE USING PHOTOGRAPHS

The studied outcrops (ERA and ERB) of the Arenazzolo Formation are located along the beach southwest of Eraclea Minoa village (Figure 1). At the outcrops, the width, amplitude and stratigraphic position of two-dimensional exposures of trough cross-sets were measured. The orientation of the plane of the exposures (i.e. plane at which troughs are cut) and the bedding attitude were measured as well. Photographs were made using a Nikon D810; their contrast and texture were enhanced in Adobe Inc (2021) Photoshop, 2021 version (Table S1).

Subtle editing of the photographs allowed for better visualisation of the sedimentary structures. Subsequently, these sedimentary structures were exploited for a qualitative palaeocurrent analysis.

3.1 | Two-dimensional palaeocurrent estimator

For the determination of palaeocurrents, an optimised procedure adopted by DeCelles and Langford (1983) was followed: sections at which the troughs are exposed in the field are grouped into four categories based on the angle between the cut-section and the trough axis (Figure 3). Each group represents an approximate range of exposure orientations and their corresponding palaeocurrent directions. Every group has distinct geometries (Figure 3).

- A. This bedform is perpendicular to the trough axis (Figure 3A). The infilling laminae of the trough are typically concentric and are to a large degree conformable with the base of the trough. The foresets are not, or only slightly, truncated by the trough base.
- B. This bedform is oriented slightly oblique at a 30° angle to the trough axis (Figure 3B). Any degree of obliquity will result in a widening of the trough base. An oblique cut generates an asymmetric structure in which foresets at one side are truncated by the trough, while they are at the other side concentric and conformable with the trough base.
- C. This bedform resembles B (Figure 3B) but shows a higher degree of foreset truncation at the base of the trough, corresponding with a smaller angle of the exposure plane with respect to the trough axis (Figure 3C).

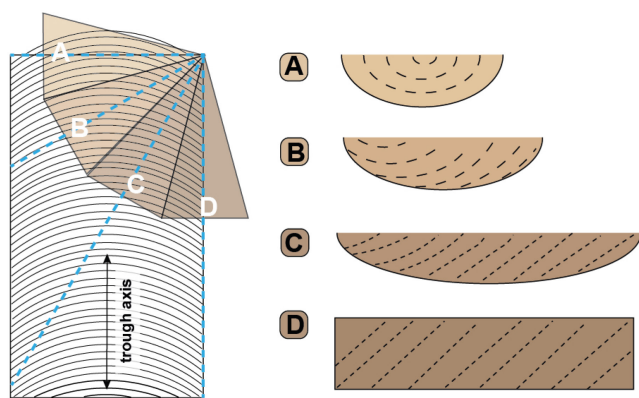


FIGURE 3 Conceptual relationship between a trough with concentric laminae and their appearance at different angles in an outcrop. Four different ranges of trough exposures are defined in groups (A–D). The corresponding two-dimensional cross-sections are depicted. Note that geometries are grouped within a bin size of 30°.

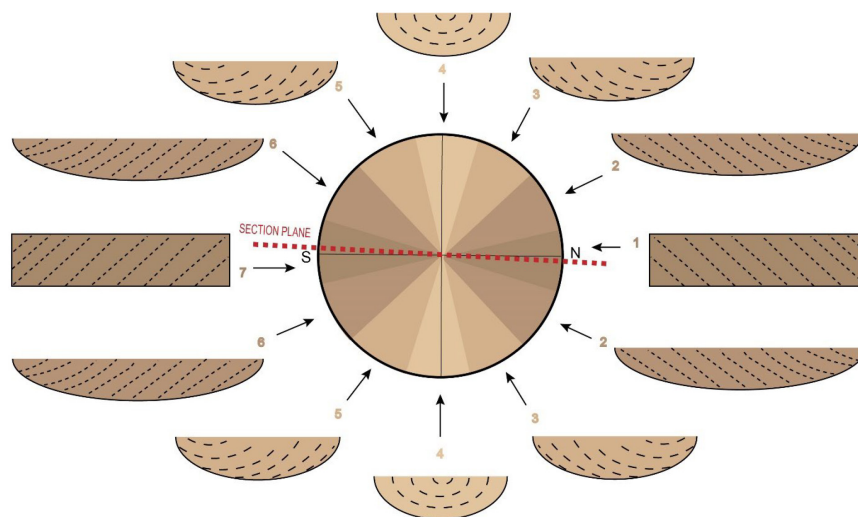
D. Longitudinal cuts are parallel to the trough axis and contain a uniform series of foresets that downlap onto the trough base (Figure 3D). Longitudinal exposures can be hard to distinguish from any type of two-dimensional exposure of tabular cross-stratification. However, when encountered within a trough cross-stratified coset, it can be assumed that this geometry also represents trough cross-stratification.

These four groups can be split into seven groups when incorporating the orientation of the foresets (Figure 4). For instance, a slightly oblique section (group B) can have a component of preferred dip direction towards either the left or the right. Therefore, this group represents two different geometries and can be split into two subgroups. In ERA, a total of 98 sets were measured, 74 sets of the same coset that has been subjected to AMS and 24 sets from a correlative coset (ERB) 269 m apart (Figure 5). This coset was correlated to the other cross-stratified cosets after constructing a fence diagram. The two possible palaeocurrent direction ranges determined with this method are plotted in rose diagrams with a non-linear frequency scale according to the procedure of Nemec (1988). In addition, the approximate means of the cosets are calculated using the central direction of each group and the number of counts in each group (Supplementary Material S2).

3.2 | Testing results with AMS measurements

Samples were collected using a portable battery-powered drill. In total, 50 standard size (25 mm diameter) cores were drilled at five sites from the same outcrop. The bedding attitude was measured using a standard compass and a 3.4° counter clockwise declination correction was applied (BGS, 2023). Four sites were drilled from various stratigraphic levels in one coset of trough cross-stratified fine sandstone (Figure 5). The remaining site was drilled in a structureless mudstone underlying the cross-bedded sandstone. The mudstone was not subjected to palaeocurrent analyses but was studied to gain an indication of a possible tectonically induced fabric. Cores were cut in the laboratory into specimens of 22 mm height. The AMS measurements were performed using an AGICO Kappa Bridge MFK1-Fa instrument (AGICO Inc., Brno, Czech Republic) at room temperature at the palaeomagnetic laboratory Fort Hoofddijk (Utrecht University, The Netherlands). Specimens were measured in an applied field strength of 200 Am⁻¹ at 976 Hz, after calibration and sample holder correction. Measurements were performed using the spinning specimen method; susceptibility is volume normalised. All

FIGURE 4 Seven geometry subgroups of trough cross-strata and their corresponding range of palaeocurrent directions in a rose diagram. The orientation of the plane of the outcrop is indicated by the red dashed line. Photographs were made perpendicular to the plane of cross-section (dashed line). Note west is up.



specimens were measured within 1 month after their collection in the field.

3.3 | Petrographic analysis

Thin sections polished from oriented samples from the coset corresponding to the AMS analysis have been studied to provide mineralogical constraints. The fabric, textures and compositions were studied with a petrographic microscope and a tabletop scanning electron microscope (TTSEM) at Utrecht University (Netherlands). The scanning electron microscope allowed for spot analysis using energy-dispersive X-ray spectroscopy. Spot analysis was done to identify the elemental composition of individual grains. Prior to TTSEM, three polished thin sections were carbon coated to prevent electric conduction. These three thin sections were selected from a total of eight that were first analysed using a petrographic microscope.

4 | RESULTS

The Arenazzolo Formation consists of semi-consolidated fine-grained sandstones with planar-laminated, structureless and trough cross-laminated cosets (Figure 5). Bioturbation is nearly absent (Rodríguez-Tovar et al., 2023) and no tectonic or diagenetic structures (e.g. deformation bands, veins or pressure solution structures) have been observed.

4.1 | Palaeocurrent estimation

The outcrop face of the trough cross-stratified coset ERA has a strike of 2° (Figure 1). The troughs have a typical average width of 6 cm, although some range up to 14 cm (Figure 6). The troughs were categorised based on their

geometry from photographs according to the procedure explained previously. In total, 74 sets were categorised from ERA. This yields two palaeocurrent groups in rose diagrams; possibility A has a dominant eastward-oriented palaeocurrent direction, while possibility B has a dominant westward-oriented palaeocurrent direction (Figure 7).

To determine the actual transport direction, a second correlative trough cross-stratified coset from section ERB was analysed (Figures 5 and 7). This correlative coset has an outcrop strike of 78° and contains mostly oblique trough cross-stratified sets. The typical average width is ca 10 cm and can range up to 30 cm. These sets correspond to either a north-eastward or a south-eastward palaeocurrent direction (Figure 7D).

4.2 | Anisotropy of magnetic susceptibility

The bulk susceptibility varies between 100×10^{-6} SI in the mudstone and 280×10^{-6} SI in the sandstones (Table S3). The AMS ellipsoid of all sites is triaxial with three well-developed clusters on the stereograms (Figure 8A through E). These clusters give rise to a weak magnetic lineation ($L = 1.011$). Next, the four sites of the Arenazzolo sandstones are merged to represent a composite projection of one coset (Figure 8F). It shows that both K_{\max} and K_{int} are not exactly parallel to the bedding plane, and K_{\min} is tilted off-vertical (Figure 8). The azimuth of the mean lineation of the maximum principal axis is 145° in stratigraphic coordinates. Moreover, the corrected degree of anisotropy (P_j) is ca 7%. One specimen corresponds to a negative shape parameter (T) and has been rejected from the dataset (Table S4).

The mudstone has the K_{\max} clustered in the west, at a different direction compared to the Arenazzolo (Figure 8E). The azimuth of the mean lineation of the maximum

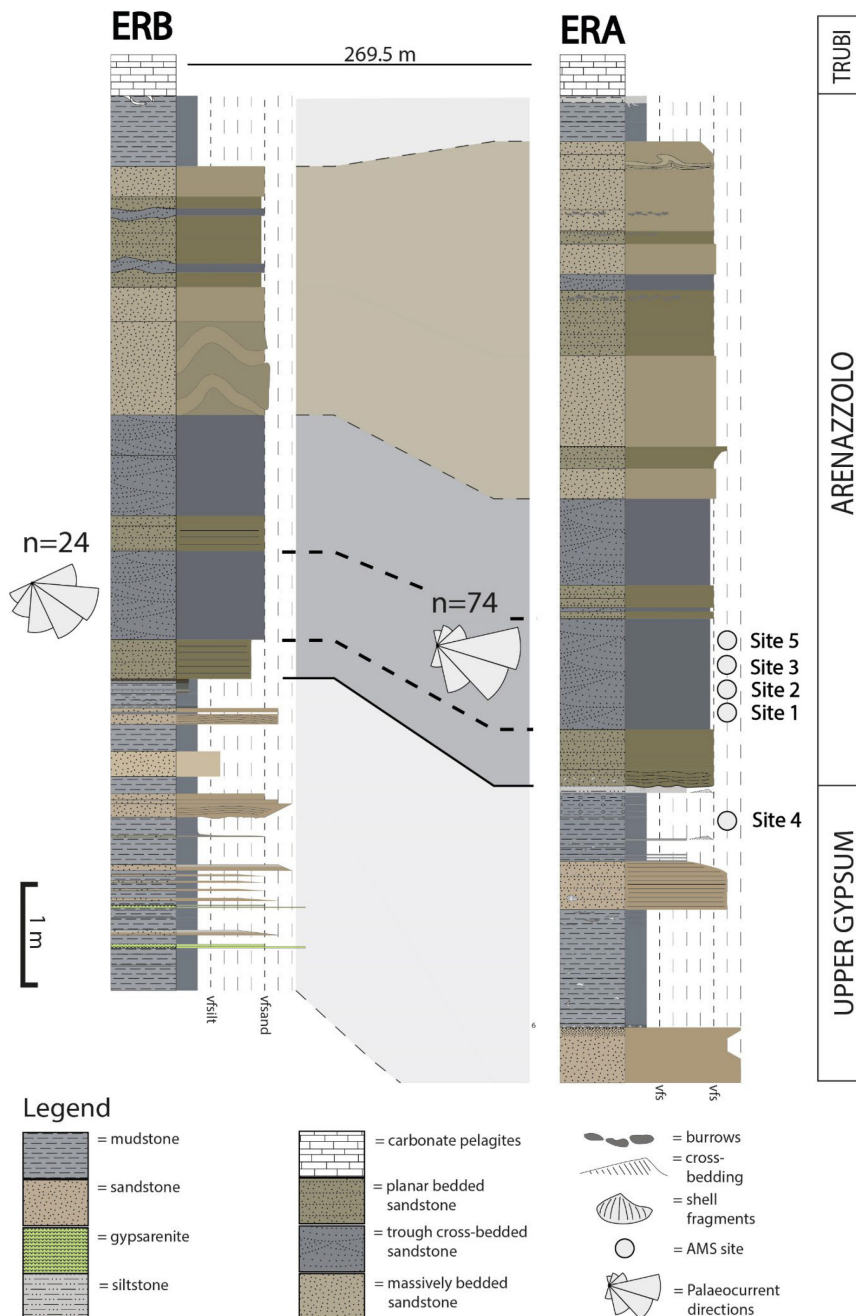


FIGURE 5 Stratigraphic logs with lithostratigraphic correlation of ERA and ERB. The correlated studied cosets are indicated with a red dotted line. Modified from van Dijk et al. (2023).

principal axis of the mudstone is 95° in stratigraphic coordinates (Figure 8E). Both the mean magnetic lineation ($L = 1.006$) and the corrected degree of anisotropy ($P_j = 3\%$) are lower in the mudstone than in the Arenazzolo sandstones (Supplementary Material S5).

4.3 | Petrographic results

Thin-section micrographs show a mixture of bioclasts, lithoclasts and quartz contained in a clayey matrix (Figure 9). Cement is lacking and a diagenetic or ichnofabric is unobserved (Supplementary Material S6 and S7). The lithoclasts mainly consist of phyllosilicates with a rightwards downdip

direction (Figures 9 and 10) parallel to foreset laminae (Figure 9C). Alternating 0.5–3 mm thick bands are present along the foreset laminae consisting of layers with concentrated quartz grains with less matrix and bands of concentrated lithoclasts with more clayey matrix (Figure 9C). The grain fabric is foliated and heavy minerals (e.g. magnetite) are equant and randomly dispersed (Figure 10).

5 | COMPARISON OF RESULTS AND TECHNIQUES

The goniometric relationship of troughs with the orientation of the cut results in an ambiguity of oblique and

FIGURE 6 (A) Photograph of trough cross-stratified coset. (B) Interpretation of trough cross-stratified coset visible in the photograph. The interpreted geometry of the troughs serves to determine the palaeocurrent directions.

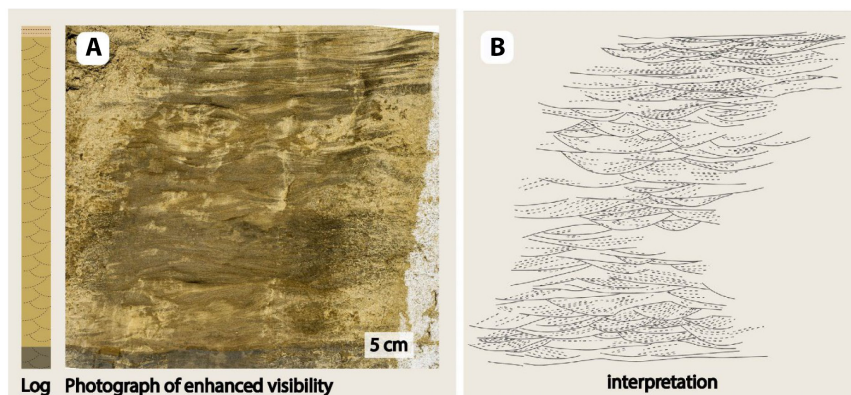
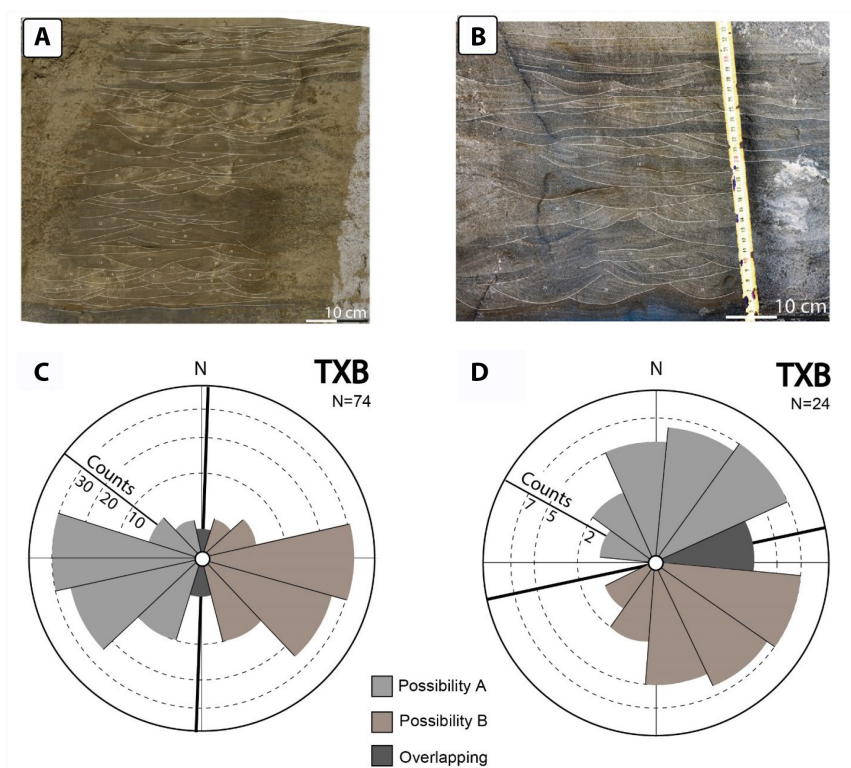


FIGURE 7 Palaeocurrent estimate from two lithostratigraphic correlated outcrops. (A) Photograph of cross-stratified coset ERA. (B) Photograph of the correlated trough cross-stratified coset ERB. (C) Rose diagram (bin size 30°) indicating the estimated palaeocurrent range corresponding to photograph A. The black line indicates the outcrop plane. (D) Rose diagram (bin size 30°) indicating the estimated palaeocurrent range of ERB. Note two possibilities are provided of which only one represents the actual palaeocurrent. The overlapping ranges pertain to both possibilities.



perpendicular cut troughs (Figure 2). Therefore, a coset must be compared with a correlative coset exposed at a different angle (Figure 7). Under the premise that the flow is not bimodal bipolar (i.e. it comes in two directions at a mutual 180° angle), the direction towards the ESE is interpreted to be the true palaeocurrent direction, because this is the overlapping palaeocurrent direction (Figure 7). The assumption of a non-bimodal bipolar flow seems valid as no evidence for such flow behaviour (e.g. tidal facies) exists. The data corresponding to the ESE population have a mean direction of $115.43^\circ \pm 25^\circ$, with a sample mean of 108.5° for ERA and of 136.75° for ERB (Figure 11). Deriving palaeocurrent directions from two-dimensional troughs comes with an uncertainty range; a computational model demonstrated that oblique cut troughs can estimate the palaeocurrent direction to

within an $ca\ 25^\circ$ error range (DeCelles & Langford, 1983). Hence, the procedure delivers an estimate rather than a precise determination of the palaeocurrent direction.

The palaeocurrent direction inferred from the magnetic fabric measured at Eraclea Minoa is unimodal. The clustering of the K_{max} with a slightly off-vertical K_{min} is characteristic for a current induced fabric with imbrication (Tauxe, 2010). Imbrication results in offset of the K_{min} from the vertical, typically towards the palaeocurrent direction with a 10–20° angle (Taira, 1989). The K_{max} is clustered resulting in a strong magnetic lineation ($L=1.011$). Like the trough cross-strata photographic technique, the AMS approach comes with an inherent uncertainty. The maximum deviation within the 95% confidence ellipse is 19° from the mean AMS direction. This provides a mean palaeocurrent direction towards the south-east with an angle of $145^\circ \pm 19^\circ$ to north.

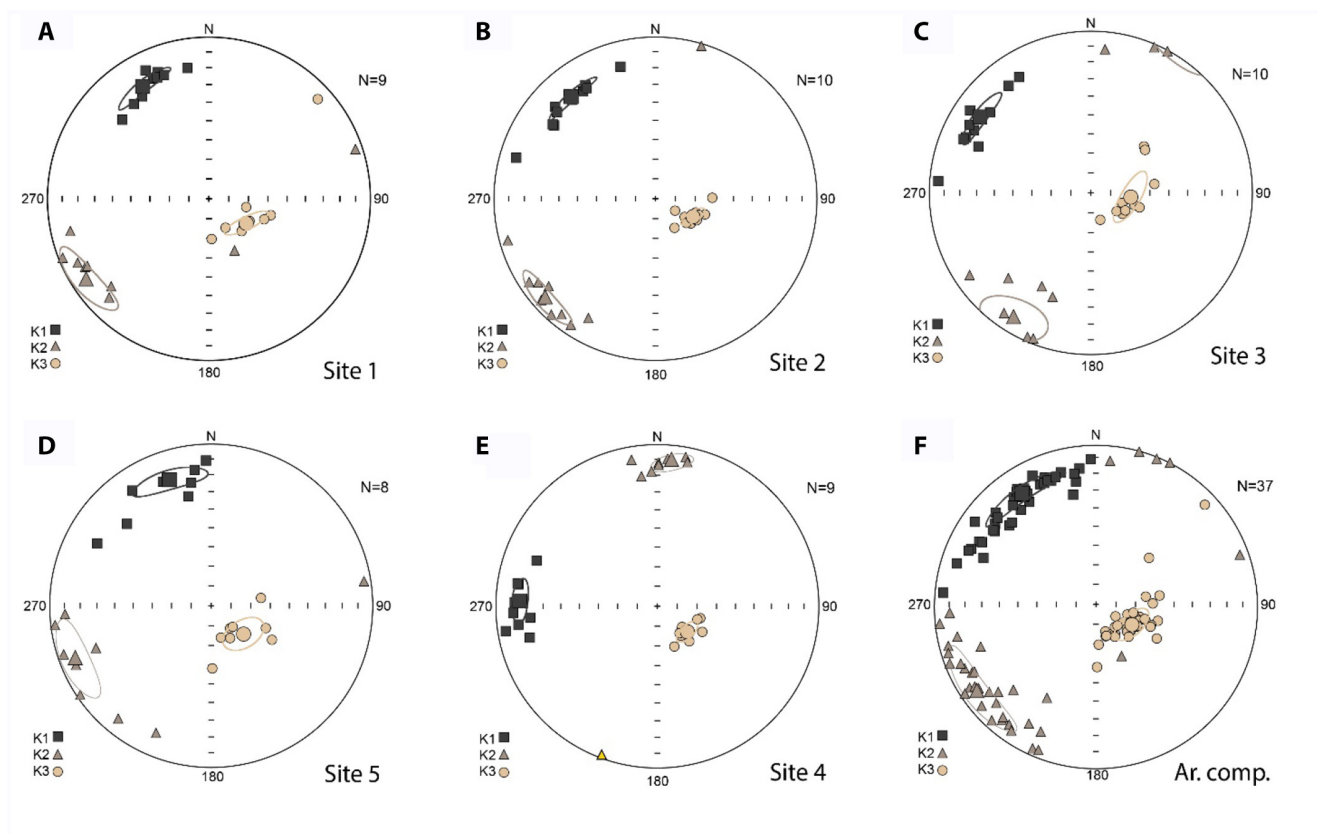


FIGURE 8 Lower hemisphere equal area projections indicating the directions of the three principal AMS axes. The square indicates the K_{\max} , the triangle indicates the K_{int} and the circles indicate the k_{\min} . (A–F) are projections after bedding correction. Note panel F (Ar. Comp.) shows the merged Arenazzolo sandstone sites (panels A–D), while panel E shows the mudstone site.

Comparison of the results of both techniques implies that the mean direction recovered from photographs of trough cross-strata falls within the bounds of uncertainty of the AMS approach (Figure 12). This agreement corroborates the accuracy of palaeocurrent estimates using the geometry of trough cross-stratification, despite its somewhat inherently low precision. Nevertheless, an up to 30° deviation in grain fabric and flow direction is considered reasonable in palaeocurrent analysis (Sakai et al., 2002), suggesting that any palaeocurrent analysis comes with an inherently low precision. The broad agreement between results from both techniques mutually validates AMS and the two-dimensional trough cross-strata photographic technique as a palaeocurrent estimator.

6 | DISCUSSION

6.1 | Complications of using two-dimensional troughs

There are some complications with estimating palaeocurrent directions from two-dimensional troughs. First, the approach assumes that troughs are filled symmetrically.

According to Slingerland and Williams (1979), about 50%–70% of foreset laminae are indeed symmetrically dispersed about the trough axis. Therefore, the basic assumption is generally valid, albeit it comes with an uncertainty range (DeCelles & Langford, 1983). A second complication is that non-cylindrically filled troughs cannot be analysed (DeCelles & Langford, 1983). This problem must be overcome statistically as *ca* 80% of all troughs exposed are cylindrical (Slingerland & Williams, 1979). Therefore, a sufficiently large dataset minimises this problem. Moreover, as with all types of palaeocurrent analyses, a bias can be introduced as a result of preservation potential. Structures formed by stronger currents could never have been preserved, as they erode rather than preserve sediments.

The addition of using photographs to the procedure of DeCelles and Langford (1983), as presented here, has advantages. First, analysing photographs forces one to interpret all troughs, whereas the analysis of the outcrop is prone to bias, as troughs that are more recognisable (e.g. strike sections) are probably to be preferred over structures with a complex morphology or poorer exposure. Second, edited photographs (by adjusting brightness and contrast) allow for better visualisation of sedimentary structures, which helps with the interpretation of the trough geometry. Third, considerably

FIGURE 9 (A, C, E) Plane-polarised light (PPL) micrographs of trough cross-stratified coset and (B, D, F) illustrations depicting a selection of grains from corresponding micrograph. Micrographs show grains in a clayey matrix with a preferred orientation of phyllosilicates with rightwards downdip direction and a compositional banding along successive foreset laminae.

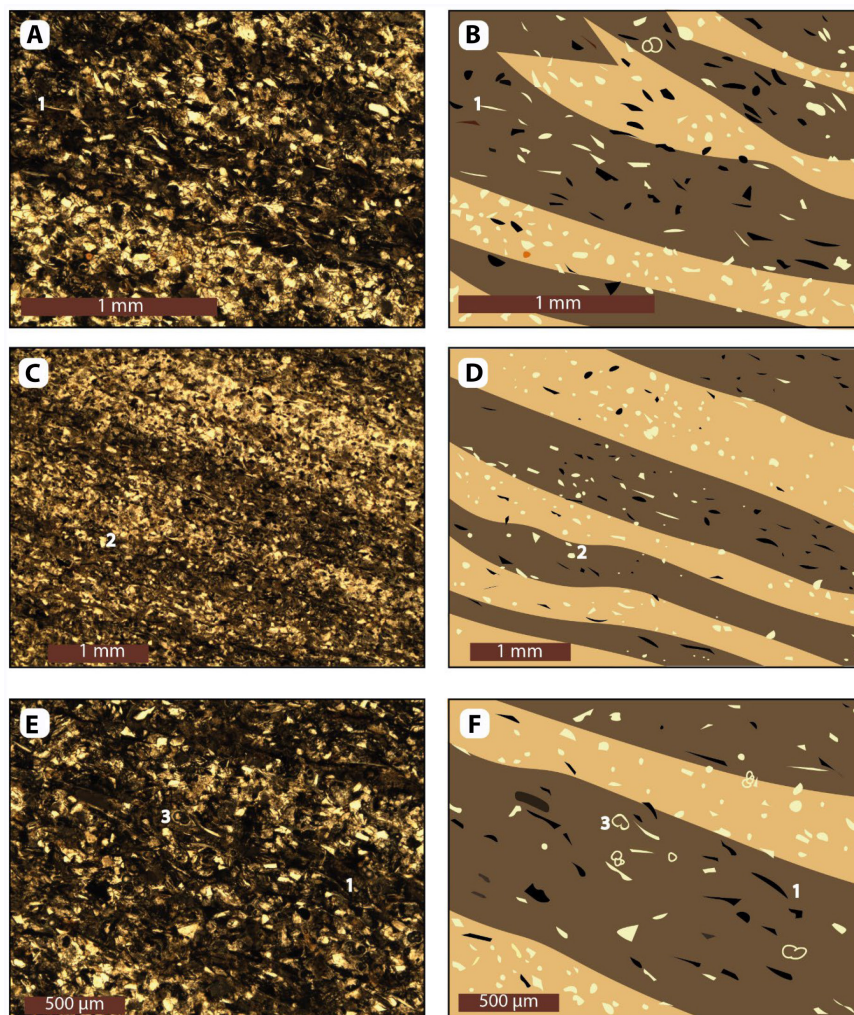
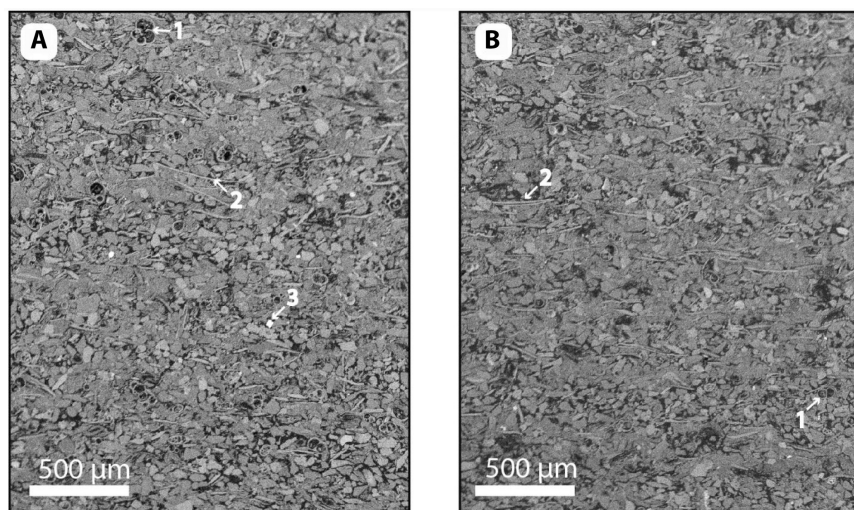


FIGURE 10 (A, B) Backscattered electron micrographs showing foliated grain fabric of the trough cross-stratified coset. (1) Foraminifer bioclast, (2) phyllosilicate, (3) heavy mineral in (A). Note that grains with high reflectance values (i.e. heavy minerals) are equant and randomly dispersed.



less time consuming trough measuring work in the field is required, the photographs suffice. Finally, the palaeocurrent analysis becomes more reproducible and transparent. Thus, the addition of photographs to the procedure of DeCelles and Langford (1983) helps to acquire a trough dataset as comprehensive as possible.

6.2 | Magnetic fabric pitfalls

Generally, grains are aligned with the direction of the depositional current. Nevertheless, if the flow is vigorous, elongated grains orient themselves perpendicular

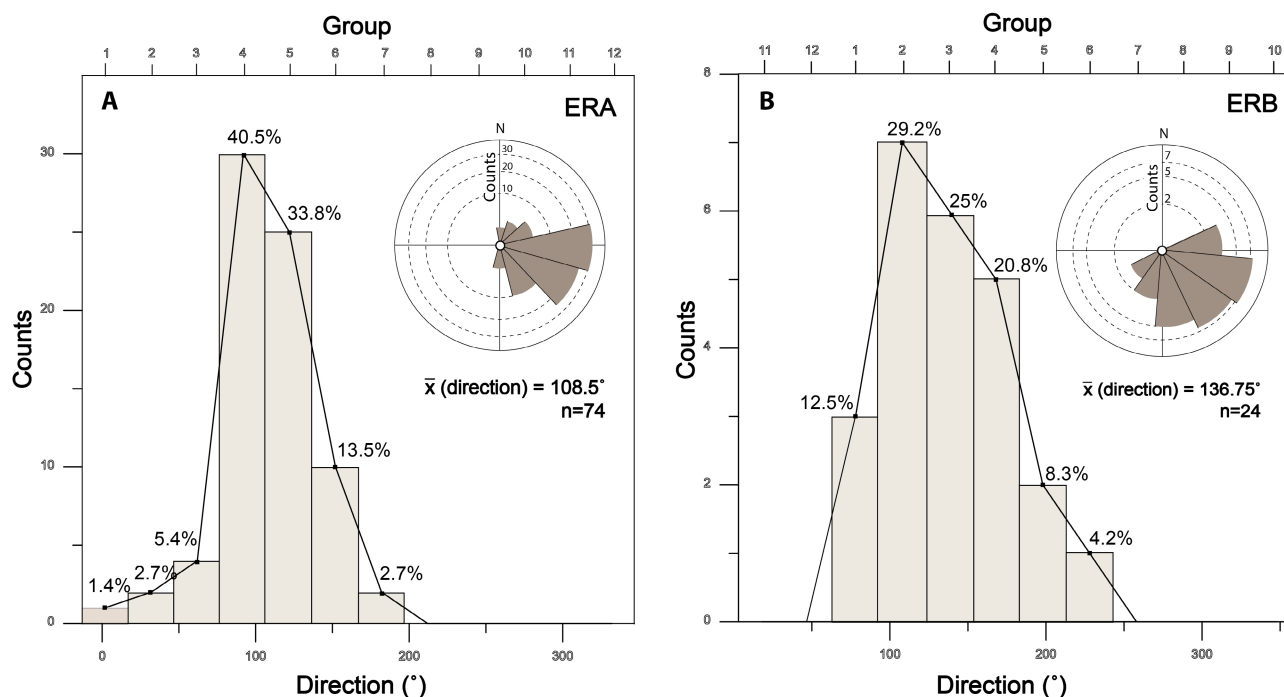


FIGURE 11 Histograms showing categorical data derived from two-dimensional trough cross-strata and their statistics. (A) Palaeocurrent distribution of ERA and (B) palaeocurrent distribution of ERB. Categories and their corresponding central direction (°) are plotted along the X-axis and the number of counts are plotted along the Y-axis. Note that counts are plotted along a non-linear axis in rose diagrams to correct for graphic distortion of the histogram (Nemec, 1988). Formulas used to calculate means are appended ([Supplementary Material S8](#)).

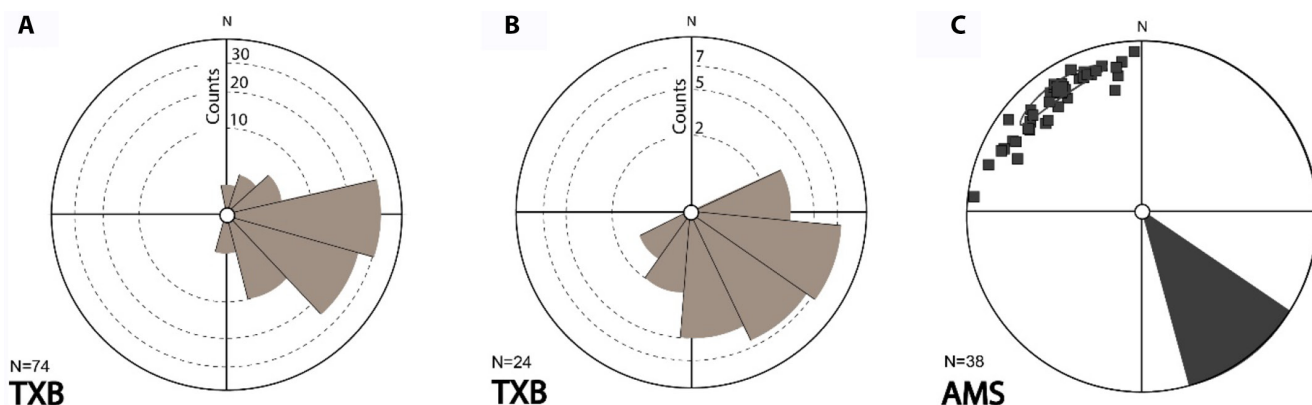


FIGURE 12 (A, B) Rose diagrams indicating approximated palaeocurrent directions from trough cross-bedded cosets. Trough cross-stratification is denoted as TXB. (C) AMS-derived palaeocurrent directions after interpreting K_{\max} current-parallel with grain-long axes. The range is defined by the 95% confidence ellipse. Python script for plotting the rose diagram is appended ([Supplementary Material S9](#)).

to the current due to the rolling of the grains (Ellwood & Ledbetter, 1977). This flow-perpendicular fabric is expected at the base of coarse-grained turbidites where energy levels were substantially high. These primary fabrics can be altered due to deformation, thereby obscuring the sedimentary fabric. In this study, the magnetic fabric of the Arenazzolo sandstones was compared with the magnetic fabric of the underlying mudstones (Figure 8E) and the overlying pelagites of the Trubi Formation from

literature (Duermeijer & Langereis, 1998). The magnetic fabric of the underlying mudstones and the overlying Trubi pelagites are in mutual agreement and may correspond to a north-to-south compression, whereas the intercalated Arenazzolo sandstones have deviating magnetic fabrics (Figure 8). Hence, the magnetic fabric of the Arenazzolo sandstones probably expresses its depositional fabric and is suitable for palaeocurrent estimation.

Besides tectonic overprinting of the depositional fabric, some other complexities can arise with palaeocurrent determination using AMS. For instance, some magnetic fabrics may have a better preservation potential than others. Magnetic fabrics predominantly reside in elongated flaky phyllosilicates (e.g. biotite and muscovite) within the sediment (Martín-Hernández & Hirt, 2001). The larger troughs that are produced by stronger currents contain less elongated phyllosilicates due to the effect of winnowing. Therefore, the palaeocurrent direction derived from AMS may represent only the palaeocurrent direction of the weaker currents. If there is friction between water masses, the strength of a current influences the direction of the current. Therefore, the magnetic fabric can be somewhat different from the palaeocurrent direction of the troughs that lack this lithological effect.

Moreover, a bias in the AMS could occur as a result of an oblique grain fabric. An oblique grain fabric has been reported in microscope studies (Potter & Mast, 1963; Spotts, 1964; Sestini & Pranzini, 1965; Scott, 1967; Onions & Middleton, 1968; Parkash & Middleton, 1970; Davies & Walker, 1974; Johansson, 1976; Channell et al., 1979). Likewise, AMS studies regularly contain an enigmatic but consistent offset with visible sedimentary structures in the same strata (Crimes & Oldershaw, 1967; Felletti et al., 2016). This offset was also observed in empirical studies integrating flume experiments and AMS (Rees & Woodall, 1975). A reassessment of a grain fabric study by Baas et al. (2007) showed that there is a statistically significant oblique flow mode, whereby the mean grain long axis tends to align at an average 40° angle with respect to the current direction. Baas et al. (2007) argues that oblique fabrics may be more common than literature suggests since minor offsets could have been ignored and thus remain unreported. Several mechanisms that create oblique fabrics are proposed: (1) spatial current variability (Parkash & Middleton, 1970; Davies & Walker, 1974), such as current interaction (e.g. superimposed downslope and along-slope currents; Scott, 1967); (2) incomplete reorientation of a flow-aligned fabric into a rolling fabric (Hughes et al., 1995); or (3) soft sediment deformation (Onions & Middleton, 1968). All three mechanisms are common depositional processes and hence, an oblique fabric should be accounted for when using AMS.

6.3 | Magnetic mineralogy

The mineralogy (i.e. content, crystal sizes and crystal shapes) and hence diagenesis affect the magnetic fabric and can cause counterintuitive AMS results (Borradaile et al., 2012). To exclude potential mineralogical pitfalls and postulate a magnetic carrier, thin sections were analysed.

The thin section micrographs show a foliated grain fabric with large (up to 500 µm) phyllosilicates oriented along foreset laminae (Figures 9 and 10). Phyllosilicates generally exhibit a strong control on the magnetic fabric alongside trace amounts of magnetite (Parés, 2015). In particular, iron-bearing and magnesium-bearing phyllosilicates can dominate the magnetic fabric (Borradaile et al., 1986). In micrographs of the Arenazolo Formation, phyllosilicates are abundant, while heavy minerals (e.g. magnetite) have an isometric shape and are randomly dispersed (Figure 10). Therefore, the dominant carriers for the low-field AMS of the Arenazolo Formation are interpreted to be dominated by phyllosilicates, while the contribution of magnetite is probably marginal at best (see Biedermann & Bilardello, 2021).

Besides phyllosilicates, micrographs reveal inclined compositional bands of alternating diamagnetic and paramagnetic minerals (Figure 9). These millimetre-thick bands correspond to the foreset laminae of the trough cross-stratification and arise from avalanches down the lee side of ripple crests (Schieber & Southard, 2009). Compositional banding arising from such preferential concentrations of magnetic grains along specific planes can contribute to a distribution anisotropy (Biedermann & Bilardello, 2021). Since the compositional bands correspond with the successive foreset laminae, the distribution anisotropy arising from these bands relates to the palaeocurrent direction, apart from a preferred grain alignment. Therefore, these compositional bands may add to the magnetic fabric and describe hydrodynamic conditions.

6.4 | Reconstructing depositional environments using palaeocurrents

Palaeocurrent directions are important for palaeoreconstructions and can help to interpret the depositional environment of sedimentary deposits. For example, contourites characteristically correspond to palaeocurrents directed along a depositional slope. Contourites are underrepresented in the geological rock record (Stow & Lovell, 1979; Shanmugam, 2017, 2021; Stow & Smillie, 2020). Hence, more methods to conduct palaeocurrent analysis can help to fill the existing gap in the stratigraphic record by identifying contourites. The mutual validation of the two techniques presented here demonstrates that these techniques are good candidates to alleviate existing controversy around contourites (Shanmugam, 2000, 2008; Stow & Smillie, 2020).

In summary, the photograph technique using two-dimensional troughs combined with AMS is a powerful tool for palaeocurrent analysis. The magnetically inferred palaeocurrent direction typically corroborates the visually determined palaeocurrent direction. Conversely, the

palaeocurrent estimates from troughs can confirm the preservation of the primary magnetic fabric. Moreover, specimens used to measure AMS can also be used for the measurement of the natural remanent magnetisation. By doing so, the orientation of the plane at which the core was cut can be fully restored by undoing post-depositional possible tectonic rotation. The application of both AMS and the geometry of two-dimensional trough cross-strata offers possibilities to conduct palaeocurrent analysis on outcrops and oriented cores.

7 | CONCLUSIONS

Photographs of two-dimensional exposures of trough cross-strata from vertical outcrops can be used to approximate palaeocurrent directions. In this study, palaeocurrent directions are estimated by analysing photographs of two-dimensional trough cross-strata made perpendicularly to vertical outcrops. This approach is an optimisation of the procedure of DeCelles and Langford (1983) with the addition of photographs and the AMS methodology. The main advantage of using photographs is that one is forced to interpret all structures present in the outcrop, rather than only the best recognisable ones. In addition, photographs allow for better visualisation using software and they improve the reproducibility of the palaeocurrent analysis. As a result, photographs provide a more complete interpretation of trough cross-stratified cosets, thereby preventing a bias. Furthermore, the AMS method can be added as an independent control point to corroborate results. It has been demonstrated here that palaeocurrent estimates of the Arenazzolo Formation derived from AMS are in broad agreement with palaeocurrent estimates derived from the geometry of two-dimensional troughs. This agreement confirms the validity of both methods as palaeocurrent indicators.

ACKNOWLEDGEMENTS

This research was carried out in collaboration with the Department of Earth Sciences at Utrecht University and 'The Drifters' Research Group at Royal Holloway University, London. The research of the UU-team was supported by the project SALTGIANT, which has received funding from the European Union's Horizon 2020 research and innovation program under the Horizon Europe 2020 grant agreement no. 765256. We wish to thank Maxim Krasnoperov, Rosa de Boer and Cor Langereis for their support and advice.

CONFLICT OF INTEREST STATEMENT


The authors declare they have no affiliations with or involvement in any organisation or entity with financial or non-financial interest in the work submitted.

DATA AVAILABILITY STATEMENT

The data that support the findings of this study are available from the corresponding author upon reasonable request.

ORCID

Jasper Maars  <https://orcid.org/0009-0005-2803-7037>

Francisco J. Rodriguez-Tovar  <https://orcid.org/0000-0002-1400-2715>

REFERENCES

- Adobe Inc. (2021) Adobe Photoshop, San Jose, CA. <https://www.adobe.com/products/photoshop.html>
- Allen, J.R.L. (1963) The classification of cross-stratified units. With notes on their origin. *Sedimentology*, 2(2), 93–114. <https://doi.org/10.1111/j.1365-3091.1963.tb01204.x>
- Amajor, L.C. (1987) Palaeocurrent, petrography and provenance analyses of the Ajali sandstone (Upper Cretaceous), south-eastern Benue Trough, Nigeria. *Sedimentary Geology*, 54(1–2), 47–60. [https://doi.org/10.1016/0037-0738\(87\)90003-0](https://doi.org/10.1016/0037-0738(87)90003-0)
- Baas, J.H., Hailwood, E.A., McCaffrey, W.D., Kay, M. & Jones, R. (2007) Directional petrological characterisation of deep-marine sandstones using grain fabric and permeability anisotropy: methodologies, theory, application and suggestions for integration. *Earth-Science Reviews*, 82(1–2), 101–142.
- Bache, F., Popescu, S.M., Rabineau, M., Gorini, C., Suc, J.P., Clauzon, G., Olivet, J.L., Rubino, M.C., Melinte-Dobrinescu, F., Estrada, L., Londeix, R., Armijo, B., Meyer, L., Jolivet, G., Jouannic, E., Leroux, D., Aslanian, A.T.D., Reis, L., Mocochain, Dumurdzanov, N., Zagorchev, I., Lesić, V., Tomić, D., Namik Çağatay, N., Brun, J.P., Sokoutis, D., Csato, I., Ucarkus, G. & Çakir, Z. (2012) A two-step process for the reflooding of the Mediterranean after the Messinian Salinity Crisis. *Basin Research*, 24(2), 125–153.
- BGS. (2023, April 14) International Geomagnetic Reference Field 13th generation. Available from: http://www.geomag.bgs.ac.uk/data_service/models_compass/igrf_calc.html [Accessed 11 April 2023]
- Biedermann, A. & Bilardello, D. (2021) Practical magnetism VII: Avoiding common misconceptions in magnetic fabric interpretation. *The IRM Quarterly*, 31(3), 1–18.
- Borradaile, G., Mothersill, J., Tarling, D. & Alford, C. (1986) Sources of magnetic susceptibility in a slate. *Earth and Planetary Science Letters*, 76, 336–340. [https://doi.org/10.1016/0012-821X\(86\)90084-1](https://doi.org/10.1016/0012-821X(86)90084-1)
- Borradaile, G.J. (1991) Correlation of strain with anisotropy of magnetic susceptibility (AMS). *Pure and Applied Geophysics*, 135(1), 15–29.
- Borradaile, G.J., Almqvist, B.S. & Geneviciene, I. (2012) Anisotropy of magnetic susceptibility (AMS) and diamagnetic fabrics in the Durness Limestone, NW Scotland. *Journal of Structural Geology*, 34, 54–60.
- Brolsma, M.J. (1978) Quantitative forminiferal analysis and environmental interpretation of the Pliocene and topmost Miocene on the south coast of Sicily. Doctoral dissertation, Utrecht University.
- Butler, R.W., Maniscalco, R. & Pinter, P.R. (2019) Syn-kinematic sedimentary systems as constraints on the structural response

- of thrust belts: re-examining the structural style of the Maghrebian thrust belt of Eastern Sicily. *Italian Journal of Geosciences*, 138(3), 371–389.
- Channell, J.E.T., Heller, F. & Van Stuijvenberg, J. (1979) Magnetic susceptibility anisotropy as an indicator of sedimentary fabric in the Gurnigel Flysch. *Eclogae Geologicae Helvetiae*, 72(3), 781–787.
- Cita, M.B. & Colombo, L. (1979) Sedimentation in the latest Messinian at Capo Rossello (Sicily). *Sedimentology*, 26(4), 497–522.
- Collinson, J.D. & Thompson, D.B. (1982) *Sedimentary structures*. London: George Allen and Unwin.
- Crimes, T.P. & Oldershaw, M.A. (1967) Palaeocurrent determinations by magnetic fabric measurements on the Cambrian rocks of St. Tudwal's Peninsula, North Wales. *Geological Journal*, 5(2), 217–232.
- Davies, I.C. & Walker, R.G. (1974) Transport and deposition of resedimented conglomerates; the Cap Enrage Formation, Cambro-Ordovician, Gaspe, Quebec. *Journal of Sedimentary Research*, 44(4), 1200–1216.
- DeCelles, G.P. & Langford, R.P. (1983) Two new methods of Palaeocurrent determination from trough cross-stratification. *SEPM Journal of Sedimentary Research*, 53(2), 629–642. <https://doi.org/10.1306/212f824c-2b24-11d7-8648000102c1865d>
- Duermeijer, C.E. & Langereis, C.G. (1998) Astronomical dating of a tectonic rotation on Sicily and consequences for the timing and extent of a middle Pliocene deformation phase. *Tectonophysics*, 298(1–3), 243–258.
- Ellwood, B.B. & Ledbetter, M.T. (1977) Antarctic bottom water fluctuations in the Vema Channel: effects of velocity changes on particle alignment and size. *Earth and Planetary Science Letters*, 35(2), 189–198.
- Ellwood, B.B. & Ledbetter, M.T. (1979) Palaeocurrent indicators in deep-sea sediment. *Science*, 203(4387), 1335–1337.
- Esri Inc. ArcMap (version 2.6). Software. (2016) “Aerial Imagery” [basemap]. Scale Not Given. “World Imagery”. November 19, 2022. Redlands, CA: Esri Inc.
- Felletti, F., Dall'Olio, E. & Muttoni, G. (2016) Determining flow directions in turbidites: an integrated sedimentological and magnetic fabric study of the Miocene Marnoso Arenacea Formation (northern Apennines, Italy). *Sedimentary Geology*, 335, 197–215. <https://doi.org/10.1016/j.sedgeo.2016.02.009>
- Hamblin, W.K. (1961) Micro-cross-lamination in Upper Keweenaw Sediments of Northern Michigan. *SEPM Journal of Sedimentary Research*, 31(3), 390–401. <https://doi.org/10.1306/74d70b87-2b21-11d7-8648000102c1865d>
- Harms, J.C., Southard, J.B., Spearing, D.R. & Walker, R.G. (1975) Depositional environments as interpreted from primary sedimentary structures and stratification sequences. *SEPM*, 2, 161.
- Hassold, N.J.C., Rea, D.K., Van der Pluijm, B.A., Parés, J.M., Gleason, J.D. & Ravelo, A.C. (2006) Late Miocene to Pleistocene palaeoceanographic records from the Feni and Gardar Drifts: Pliocene reduction in abyssal flow. *Palaeogeography Palaeoclimatology Palaeoecology*, 236(3–4), 290–301.
- Hiscott, R.N. & Middleton, G.V. (1980) Fabric of coarse deep-water sandstones, Tourelle Formation, Quebec. *SEPM Journal of Sedimentary Research*, 50(3), 703–721.
- Hsü, K.J., Ryan, W. & Cita, M. (1973) Late Miocene desiccation of the Mediterranean. *Nature*, 242, 240–244.
- Hughes, S.R., Alexander, J. & Druitt, T.H. (1995) Anisotropic grain fabric: volcanic and laboratory analogues for turbidites. *Geological Society, London, Special Publications*, 94(1), 51–62.
- Jelinek, V. (1981) Characterization of the magnetic fabric of rocks. *Tectonophysics*, 76, 63–67. [https://doi.org/10.1016/0040-1951\(81\)90110-4](https://doi.org/10.1016/0040-1951(81)90110-4)
- Jipa, D.C. & Olariu, C. (2013) Sediment routing in a semi-enclosed epicontinental sea: Dacian Basin, Paratethys domain, Late Neogene, Romania. *Global and Planetary Change*, 103, 193–206. <https://doi.org/10.1016/j.gloplacha.2012.06.009>
- Johansson, C.E. (1976) Structural studies of frictional sediments. *Geografiska Annaler: Series A, Physical Geography*, 58(4), 201–301.
- Lickorish, W.H., Grasso, M., Butler, R.W., Argnani, A. & Maniscalco, R. (1999) Structural styles and regional tectonic setting of the “Gela Nappe” and frontal part of the Maghrebian thrust belt in Sicily. *Tectonics*, 18(4), 655–668.
- Londeix, L., Benzakour, M., Suc, J.P. & Turon, J.L. (2007) Messinian palaeoenvironments and hydrology in Sicily (Italy): the dinoflagellate cyst record. *Geobios*, 40(3), 233–250. <https://doi.org/10.1016/j.geobios.2006.12.001>
- Manzi, V., Lugli, S., Roveri, M. & Charlotte Schreiber, B. (2009) A new facies model for the Upper Gypsum of Sicily (Italy): chronological and palaeoenvironmental constraints for the Messinian salinity crisis in the Mediterranean. *Sedimentology*, 56(7), 1937–1960.
- Martín-Hernández, F. & Hirt, A.M. (2001) Separation of ferrimagnetic and paramagnetic anisotropies using a high-field torsion magnetometer. *Tectonophysics*, 337(3–4), 209–221.
- Nemec, W. (1988) The shape of the rose. *Sedimentary Geology*, 59(1–2), 149–152.
- Onions, D. & Middleton, G.V. (1968) Dimensional grain orientation of Ordovician turbidite graywackes. *Journal of Sedimentary Research*, 38(1), 164–174.
- Parés, J.M., Hassold, N.J.C., Rea, D.K. & Van der Pluijm, B.A. (2007) Palaeocurrent directions from palaeomagnetic reorientation of magnetic fabrics in deep-sea sediments at the Antarctic Peninsula Pacific margin (ODP Sites 1095, 1101). *Marine Geology*, 242(4), 261–269.
- Parés, J.M. (2015) Sixty years of anisotropy of magnetic susceptibility in deformed sedimentary rocks. *Frontiers in Earth Science*, 3, 4.
- Parkash, B. & Middleton, G.V. (1970) Downcurrent textural changes in Ordovician turbidite greywackes. *Sedimentology*, 14(3–4), 259–293.
- Pettijohn, F.J. (1975) *Sedimentary rocks*, 2nd edition. New York: Harper and Row.
- Piper, J.D.A., Elliot, M.T. & Kneller, B.C. (1996) Anisotropy of magnetic susceptibility in a Palaeozoic flysch basin: the Windermere Supergroup, northern England. *Sedimentary Geology*, 106(3–4), 235–258.
- Popescu, S.M., Cavazza, W., Suc, J.P., Melinte-Dobrinescu, M.C., Barhoun, N. & Gorini, C. (2021) Pre-Zanclean end of the Messinian Salinity Crisis: new evidence from central Mediterranean reference sections. *Journal of the Geological Society*, 178(3), jgs2020-183. <https://doi.org/10.1144/jgs2020-183>
- Potter, P.E. & Mast, R.F. (1963) Sedimentary structures, sand shape fabrics, and permeability I. *Journal of Geology*, 71(4), 441–471.
- Potter, P.E. & Pettijohn, F.J. (2012) *Palaeocurrents and basin analysis*. Berlin, Germany: Springer Science and Business Media.

- Rees, A.I. & Woodall, W.A. (1975) The magnetic fabric of some laboratory-deposited sediments. *Earth and Planetary Science Letters*, 25(2), 121–130.
- Rodríguez-Tovar, F.J., van Dijk, G., Maars, J., Andreetto, F., Hernández-Molina, F.J. & Krijgsman, W. (2023) Ichnological analysis of the Messinian-Zanclean (Miocene-Pliocene) transition at Eraclea Minoa (Sicily): Tracemaker response to the Terminal Messinian Flood. *Palaeogeography Palaeoclimatology Palaeoecology*, 619, 111539.
- Roveri, M., Lugli, S., Manzi, V. & Schreiber, B.C. (2008) The Messinian Sicilian stratigraphy revisited: new insights for the Messinian salinity crisis. *Terra Nova*, 20(6), 483–488.
- Roveri, M., Flecker, R., Krijgsman, W., Lofi, J., Lugli, S., Manzi, V., Sierro, F.J., Bertini, A., Camerlenghi, A., De Lange, G., Govers, R., Hilgen, F.J., Hübscher, C., Meijer, P.T. & Stoica, M. (2014) The Messinian salinity crisis: past and future of a great challenge for marine sciences. *Marine Geology*, 352, 25–58.
- Sakai, T., Yokokawa, M., Kubo, Y.S., Endo, N. & Masuda, F. (2002) Grain fabric of experimental gravity flow deposits. *Sedimentary Geology*, 154(1–2), 1–10.
- Schieber, J. & Southard, J.B. (2009) Bedload transport of mud by floccule ripples—direct observation of ripple migration processes and their implications. *Geology*, 37(6), 483–486. <https://doi.org/10.1130/G25319A.1>
- Schreiber, B.C., Friedman, G.M., Decima, A. & Schreiber, E. (1976) Depositional environments of Upper Miocene (Messinian) evaporite deposits of the Sicilian Basin. *Sedimentology*, 23(6), 729–760. <https://doi.org/10.1111/j.13653091.1976.tb00107.x>
- Scott, K.M. (1967) Intra-bed palaeocurrent variations in a Silurian flysch sequence, Kirkcudbrightshire, Southern Uplands of Scotland. *Scottish Journal of Geology*, 3(2), 268–281.
- Selli, R. (1960) Il Messiniano Mayer-Eymar 1867. Proposta di un neostatotipo. *Giornale di Geologia Series*, 2, 1.
- Sestini, G. & Pranzini, G. (1965) Correlation of sedimentary fabric and sole marks as current indicators in turbidites. *Journal of Sedimentary Research*, 35(1), 100–108.
- Shanmugam, G. (2000) 50 years of the turbidite paradigm (1950s–1990s): deep-water processes and facies models—a critical perspective. *Marine and Petroleum Geology*, 17(2), 285–342.
- Shanmugam, G. (2008) Deep-water bottom currents and their deposits. *Developments in Sedimentology*, 60, 59–81.
- Shanmugam, G. (2017) The contourite problem. In: *Sediment provenance*. Amsterdam, the Netherlands: Elsevier, pp. 183–254. <https://doi.org/10.1016/B978-0-12-803386-9.00009-5>
- Shanmugam, G. (2021) The turbidite-contourite-tidalite-baroclinite-hybridite problem: orthodoxy vs. empirical evidence behind the “Bouma Sequence”. *Journal of Palaeogeography*, 10(1), 1–32. <https://doi.org/10.1186/s42501-021-00085-1>
- Slingerland, R.L. & Williams, E.G. (1979) Palaeocurrent analysis in light of trough cross-stratification geometry. *Journal of Geology*, 87(6), 724–732. <https://doi.org/10.1086/628462>
- Stow, D.A.V. & Lovell, J.P.B. (1979) Contourites: Their recognition in modern and ancient sediments. *Earth-Science Reviews*, 14(3), 251–291. [https://doi.org/10.1016/0012-8252\(79\)90002-3](https://doi.org/10.1016/0012-8252(79)90002-3)
- Stow, D. & Smillie, Z. (2020) Distinguishing between deep-water sediment facies: Turbidites, contourites and hemipelagites. *Geosciences*, 10(2), 68.
- Spotts, J.H. (1964) Grain orientation and imbrication in Miocene turbidity current sandstones, California. *Journal of Sedimentary Research*, 34(2), 229–253.
- Taira, A. & Lienert, B.R. (1979) The comparative reliability of magnetic, photometric and microscopic methods of determining the orientations of sedimentary grains. *Journal of Sedimentary Research*, 49(3), 759–771.
- Taira, A. (1989) Magnetic fabrics and depositional processes. In: *Sedimentary facies in the active plate margin*. Tokyo: TERRAPUB, pp. 43–47.
- Tarling, D. & Hrouda, F. (1993) Magnetic anisotropy of rocks. *Geological Magazine*, 132(4), 454. <https://doi.org/10.1017/S0016756800021543>
- Tauxe, L. (2010) *Essentials of Palaeomagnetism*. Berkeley, CA: University of California Press.
- Van Couvering, J.A., Castradori, D., Cita, M.B., Hilgen, F.J. & Rio, D. (2000) The base of the Zanclean Stage and of the Pliocene Series. *Episodes Journal of International Geoscience*, 23(3), 179–187.
- Van Dijk, G., Maars, J., Andreetto, F., Hernández-Molina, F.J., Rodríguez-Tovar, F.J. & Krijgsman, W. (2023) A terminal Messinian flooding of the Mediterranean evidenced by contouritic deposits on Sicily. *Sedimentology*, 70, 1195–1223. <https://doi.org/10.1111/sed.13074>
- Zhao, X., Liu, C., Wang, J., Luo, W., Du, F. & Ma, L. (2020) Provenance analyses of Lower Cretaceous strata in the Liupanshan Basin: from palaeocurrents indicators, conglomerate clast compositions, and zircon U-Pb geochronology. *Journal of Earth Science*, 31(4), 757–771. <https://doi.org/10.1016/j.gloplacha.2012.06.009>

SUPPORTING INFORMATION

Additional supporting information can be found online in the Supporting Information section at the end of this article.

How to cite this article: Maars, J., van Dijk, G., Dekkers, M.J., Hernández-Molina, F.J., Andreetto, F., Rodríguez-Tovar, F.J. et al. (2024) New palaeocurrent analysis approach from two-dimensional trough cross-strata using photographs and anisotropy of magnetic susceptibility. *The Depositional Record*, 00, 1–14. Available from: <https://doi.org/10.1002/dep2.277>